Out-of-Time-Ordered Correlation Functions

Hui Zhai
Institute for Advanced Study, Tsinghua University

Abstract

In this note I will first briefly review the short history of the out-of-time-ordered correlator (OTOC) and discuss why this can describe chaos. I will focus on a rigorous relation between the OTOC and the entropy dynamics, and discuss the implication of this relation in several different systems. I will also briefly introduce the first experimental measurement of the OTOC for local operators with a quantum simulator, and discuss the relation between the OTOC and the Loschmidt echo.

1 General Introduction of OTOC

The out-of-time-ordered correlation (OTOC) function is introduced as

$$G(t) = \langle \hat{W}^\dagger(t)\hat{V}^\dagger(0)\hat{W}(t)\hat{V}(0)\rangle, \tag{1}$$

where $\hat{W}(t) = e^{-i\hat{H}t}We^{i\hat{H}t}$. To respect the causality, the normal correlation function discussed in many-body physics textbooks before is always time-ordered. While here in the OTOC the time arguments of the operators are not ordered. Why we are interested in such a correlation function.

1.1 A Brief History of the OTOC

- The OTOC first appeared in a paper by Larkin and Ovchinnikov in 1969 in studying a disordered superconductivity problem [1]. They found that such correlator can be related to chaos in the semiclassical limit. But until recently, there is not too much discussion of chaos based on the OTOC.

- In 2013, Shenker and Stanford encountered the same correlation function in a gravity theory when they studied a problem that is initially completely unrelated to chaos, that is, the scattering of gravitational shock waves nearby a horizontal of a black hole [2, 3]. It is Kitaev who pointed out, in a talk given in KITP in 2014 [4], that what Shenker and Stanford find in the gravity theory connects to the quantum chaos in a quantum system. This builds up a remarkable connection between two very different fields. It also maybe the first time that the name "out-of-time-ordered correlation" appeared. From the exponential derivation behavior of the OTOC one can define the Lyaponov exponent for a quantum system.

- In the black hole calculation, it is found that the Lyaponov exponent is always $2\pi k_b T$. Later, it is also found that the quantum correction from the string theory always makes the Lyaponov exponent smaller [5]. Thus it leads to a conjecture that $2\pi k_b T$ is an upper bound of the Lyaponov exponent. In 2015, under certain general conditions, Maldacena, Shenker and Stanford prove that the Lyaponov exponent of a quantum system should be smaller than this bound [6]. This is now known at the MSS bound. If a quantum system is holographic dual to a gravity system with a black hole, it means that the correlators calculated from two sides are identical, hence it is natural that the Lyaponov exponent of such a system saturates the bound. But a nontrivial conjecture is the reversed statement, that is, if the Lyaponov exponent of a quantum system saturates the bound, it will be holographic dual to a black hole.

- In three talks given in KITP in 2014 and 2015, Kitaev also discussed a model generalized from a model studied by Sachdev and Ye in 1993 [4, 7]. He showed that the Lyaponov exponent of this model saturates the bound in the strong coupling limit [4, 8]. Meanwhile, this model in the same limit displays an emergent conformal symmetry and is holographic dual to a black hole [7, 8]. This model is now known as the SYK model. It is a concrete model to support above conjecture. Recently the SYK model has drawn lots of attentions from both the gravity community and the condensed matter community, and there are also lots of work studied various extensions of the SYK model [9, 10, 11, 12, 13].

- Recent works have also applied the OTOC beyond the chaotic behavior and the holographic duality, for instance, describing information scrambling and the many-body localization [14, 15, 16, 17, 18, 19, 20, 21].

- Despite of all these theories and several proposals of how to measure OTOC [22, 23, 24, 25, 26, 27], the experimental measurements of the OTOC is quite challenging. The first two experimental measurements of the OTOC appeared in 2016 using NMR [28] and ion trap [29] quantum simulators, respectively. The NMR experiment [28] measures the OTOC for local operators while the ion trap experiment [29] does not. As we will mention below, the locality of operators in the OTOC are quite important.

1.2 The OTOC and Chaotic Behavior

There are two different ways to view the relation between the OTOC and the chaotic behavior. Let us discuss them one by one:

1.2.1 Viewpoint A

The classical chaos is described by the so-called "the butterfly effect", that is, a small initial derivation will be exponentially amplified. In the classical mechanics, for example, considering q as position and p as its conjugate variable, it is

$$\frac{\partial q(t)}{\partial q(0)} = \{q(t), p(0)\} \sim e^{\lambda_{\mathrm{L}} t}. \tag{2}$$

In the paper by Larkin and Ovchinnikov [1], they replace the Poisson bracket by the commutate square in the quantum case, and defines

$$\begin{aligned} C(t) &= \langle \| [\hat{W}(t), \hat{V}(0)] \|^2 | \rangle & (3) \\ &= \langle \hat{V}^\dagger(0)\hat{W}^\dagger(t)\hat{W}(t)\hat{V}(0)\rangle + \langle \hat{W}^\dagger(t)\hat{V}^\dagger(0)\hat{V}(0)\hat{W}(t)\rangle \\ &- \langle \hat{W}^\dagger(t)\hat{V}^\dagger(0)\hat{W}(t)\hat{V}(0)\rangle - \langle \hat{V}^\dagger(0)\hat{W}^\dagger(t)\hat{V}(0)\hat{W}(t)\rangle. & (4) \end{aligned}$$

The first two terms in Eq. 4 are the normal correlations while the last two terms are the OTOC.

Now we first introduce a concept of "the separation of the time scales". t_{d} denotes the dissipation time, that is defined as the time scale when the

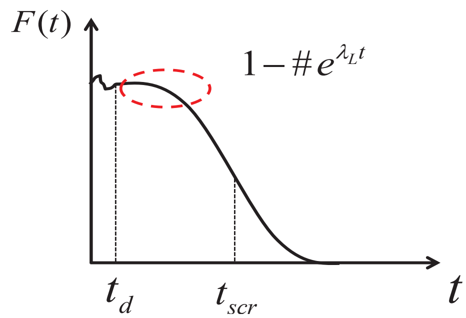

Figure 1: Schematic of a typical behavior of the normalized OTOC, which shows the separation of time scales.

normal correlation becomes separable, i.e

$$\langle V^\dagger(0)\hat{W}^\dagger(t)\hat{W}(t)\hat{V}(0)\rangle = \langle V^\dagger(0)\hat{V}(0)\rangle\langle W^\dagger(t)\hat{W}(t)\rangle. \tag{5}$$

Why Eq. 5 defines the dissipation time ? Considering a normalized quantum state $|\Psi\rangle$ and a local operator $\hat{V}$, $\hat{V}(0)$ changes the quantum state from $|\Psi\rangle$ to $\hat{V}|\Psi\rangle$ at time $t = 0$. After certain time t_d, this local change dissipates, and since $\hat{V}$ only changes few local degree of freedom in the thermodynamic degree of freedom of the system. Thus, once the excitation $\hat{V}(0)|\Psi\rangle$ thermalizes, the system returns to the original state $|\Psi\rangle$, except for a normalization factor, i.e.

$$|\tilde{\Psi}\rangle = \sqrt{\langle\hat{V}^\dagger(0)\hat{V}(0)\rangle}|\Psi\rangle. \tag{6}$$

Hence, the L.H.S. of Eq. 5 becomes the expectation value of $\hat{W}^\dagger(t)\hat{W}(t)$ under $|\tilde{\Psi}\rangle$, which gives the R. H. S. of Eq. 5.

After the dissipation time t_d, $C(t)$ defined in Eq. 4 becomes

$$C(t) = \langle V^\dagger(0)\hat{V}(0)\rangle\langle W^\dagger(t)\hat{W}(t)\rangle(2 - 2\tilde{G}(t)), \tag{7}$$

where $\tilde{G}(t)$ is the normalized OTOC defined as

$$\tilde{G}(t) = \frac{\langle\hat{W}^\dagger(t)\hat{V}^\dagger(0)\hat{W}(t)\hat{V}(0)\rangle}{\langle V^\dagger(0)\hat{V}(0)\rangle\langle W^\dagger(t)\hat{W}(t)\rangle}. \tag{8}$$

It becomes clear that if $\tilde{G}(t)$ behaves as at the scrambling time t_s

$$\tilde{G}(t) = 1 - \alpha e^{\lambda_\mathrm{L} t}, \tag{9}$$

as shown in Fig. 1, $C(t)$ will grow exponentially, which is reminiscent of the classical butterfly effect defined in Eq. 2.

Hence, we should make a remark that, in order for the OTOC to describe the chaotic behavior, it requires

1. The separation of the time scales, i.e. $t_{\mathrm{s}} \gg t_{\mathrm{d}}$
2. $\hat{V}$ and $\hat{W}$ are both local operators.

Why the "separation of the time scales" is a natural assumption ? Let us consider $\hat{W}$ and $\hat{V}$ as two local operators far separated, thus, at $t = 0$ they commute with each other and $C(t) = 1$. As time t increases

$$\hat{W}(t) = \sum_{j=0}^{\infty} \frac{(it)^j}{j!} [\hat{H}, \ldots, [\hat{H}, \hat{W}], \ldots,] \tag{10}$$

if $\hat{H}$ is local, only very high order commutates in Eq. 10 generate terms that do not commute with $\hat{V}$, that is to say, only after long time $\hat{W}(t)$ becomes not commuting with $\hat{V}$ and the OTOC starts to deviate from unity. On the other hand, thermalization is a local phenomenon and only involves the local degree of freedom nearby $\hat{V}$. Thus, it is natural to assume $t_{\mathrm{d}} \ll t_{\mathrm{s}}$.

1.2.2 Viewpoint B

Considering an eigenstate $|\Psi\rangle$ operated by an operator $\hat{V}$ at $t = 0$, it is quite obvious that

$$e^{-i\hat{H}t} e^{i\hat{H}t} \hat{V} |\Psi\rangle = \hat{V} |\Psi\rangle, \tag{11}$$

which means nothing but evolving a quantum state forward by $\hat{H}$ and then backward by $-\hat{H}$ yields the same initial state. Now, let us ask, there is another operation $\hat{W}$ inserted after the forward evolution and before the backward evolution, i.e.

$$e^{-i\hat{H}t} \hat{W} e^{i\hat{H}t} \hat{V} |\Psi\rangle, \tag{12}$$

the question is after the time evolution, whether the quantum state can still return to $\hat{V}|\Psi\rangle$. To quantify this, one can naturally look at the wave function overlap between

$$\langle\Psi| \hat{V}^{\dagger} e^{-i\hat{H}t} \hat{W} e^{i\hat{H}t} \hat{V} |\Psi\rangle. \tag{13}$$

If this overlap is nearly unity, that means insetting a perturbation $\hat{W}$ during the evolution has little effect in the final state; while if this overlap rapidly decreases, given $\hat{W}$ and $\hat{V}$ are spatially far separated, this means nothing but a butterfly effect.

However, in many cases there is a trivial reason that the overlap is zero, that is, if $\hat{W}$ changes the quantum number of the state, for instance, if $\hat{W}$ is a particle creation operator. Therefore, one wants a quantum state that has same quantum number as $e^{-i\hat{H}t}\hat{W}e^{i\hat{H}t}\hat{V}|\Psi\rangle$ while locally is identical to $\hat{V}|\Psi\rangle$. We argue that the quantum state $\hat{V}e^{-i\hat{H}t}\hat{W}e^{i\hat{H}t}|\Psi\rangle$ fulfills the requirement. The first operator $e^{i\hat{H}t}$ has no effect except for a phase factor, and after operated by $\hat{W}$, the system is backward evolved. For the same consideration as "the separation of the time scales", suppose the backward evolution time is much longer than dissipation time t_{d}, the local excitation created by $\hat{W}$ has already smeared out. Similar as the argument above, the quantum state returns to the same state as $|\Psi\rangle$, then the quantum state $\hat{V}e^{-i\hat{H}t}\hat{W}e^{i\hat{H}t}|\Psi\rangle$ is locally identical to $\hat{V}|\Psi\rangle$. Thus, instead of Eq. 13, one looks the overlap between $e^{-i\hat{H}t}\hat{W}e^{i\hat{H}t}\hat{V}|\Psi\rangle$ and $\hat{V}e^{-i\hat{H}t}\hat{W}e^{i\hat{H}t}|\Psi\rangle$, which gives exactly the OTOC as $\langle\hat{W}^\dagger(t)\hat{V}^\dagger(0)\hat{W}(t)\hat{V}(0)\rangle$. In another word, the deviation of the OTOC from unity quantifies the butterfly effect.

Before concluding this part, let me make an extra remark on the chaotic behavior and the chaotic system. Of course, if a system is fully chaotic, the OTOC of any two operators will exhibit chaotic behavior. However, if the OTOC of some operator exhibits chaotic behavior, it does not mean that the whole system has to be chaotic. As we will show later, even for an integrable system, if the operators chosen in the OTOC do not correspond to the integrable of motion for the many-body system, the OTOC can still display an exponential decay behavior around the scrambling time. In that case the difference between an integrable model and a non-integrable model will manifest itself in the long-time behavior of the OTOC.

The OTOC is a subject of extensive studies recently with many ongoing works. We are not able to give a comprehensive review for the OTOC. Instead, here we introduce the relation between the OTOC and the Rényi entropy.

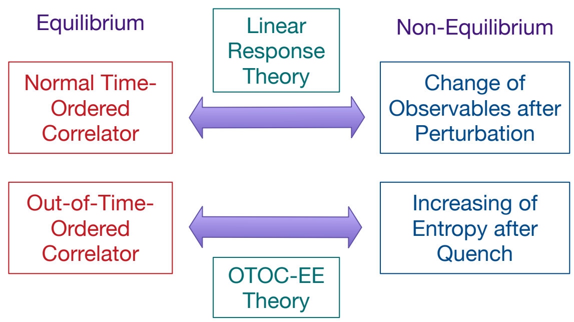

Figure 2: A comparison between the relation of OTOC and increasing of Rényi entropy after quench and the relation of normal correlator and change of observable after perturbation.

2 The OTOC and the Rényi Entropy

2.1 A General Theorem

A general theory we proved between the OTOC and the second Rényi entropy is that:

Theorem. For a system at $T = \infty$ quenched by an arbitrary operator $\hat{O}$ at $t = 0$, we divide the system into two subparts A and B and consider the second Rényi entropy $S_A^{(2)}$. The growth of this second Rényi entropy is related to the OTOC of the original equilibrium state via

$$\exp(-S_A^{(2)}) = \sum_{\hat{M}\in B} \langle \hat{M}(t)\hat{V}(0)\hat{M}(t)\hat{V}(0)\rangle_{\beta=0}, \tag{14}$$

where $\hat{V} = \hat{O}\hat{O}^\dagger$ and the summation is taken over a complete set of operators $\hat{M}$ in the part B. Here we have chosen the normalization condition for $\hat{M}$ and $\hat{O}$ as $\sum_{\hat{M}\in B} M_{ij}M_{lm} = \delta_{im}\delta_{lj}$, $\mathrm{Tr}[\hat{O}\hat{O}^\dagger] = 1$.

The proof of the theorem is in fact quite straightforward, and we put the details of the proof in the appendix. Here let us put a few remarks on the theorem:

1. Here the quench can be either a local quench or a global quench. For local quenches, for instance, for a lattice gas model, one can suddenly add one more particle in the site-i, which corresponds to the quench

operator $\hat{O} = \hat{b}_i^\dagger$; for a spin model, one can suddenly flip a spin at the site-i, which corresponds to the quench operator $\hat{O} = \hat{S}_i^-$. For global quench, it means the initial state is prepared in a many-body state that is not an eigenstate of the full Hamiltonian, for instance, a spin system with anti-ferromagnetic coupling is prepared in a ferromagnetic state. In this case, the quench operator corresponds to the projection operator to that many-body state. In any case, after the quench, the system will be in a non-equilibrium situation and the system will start to evolve in time.

2. During the time evolution, in order to study the entropy dynamics, one needs to divide the system into A and B two subparts. By tracing out the part B, one obtains the density matrix for part A as $\rho_A = \text{Tr}_B\rho$, and the second Rényi entropy is defined as $S_A^{(2)} = -\log \text{Tr}_A \hat{\rho}_A^2$.

3. The L.H.S. of Eq. 14 is a non-equilibrium property. For the L.H.S. one has the freedoms to choose any quench operator and to choose any way to divide the system into A and B. But once these two choices are made, the R.H.S. are completely fixed. In the R.H.S., $\hat{V}$ has to be taken related to the quench operator as $\hat{O}\hat{O}^\dagger$, and $\hat{M}$ has to be taken a set of complete operators in the subpart B. For instance, for a spin-1/2 model, if B is just a single-site, then $\hat{M}$ should take $\sigma_{x,y,z}$ and identity operator.

4. Eq. 14 in fact gives a relation between the OTOC in equilibrium and entropy dynamics in non-equilibrium. This is in fact reminiscent of the linear response theory, which relates the normal time-ordered correlator to the change of physical observables after a perturbation. That is in fact how the normal correlators are experimentally measured in condensed matter system, such as ARPES and neutron scattering. It is natural that the normal time-ordered correlator is related to observables because the time-order obeys causality, while the out-of-time-ordered correlator does not obey causality and surely can not be related to normal observables. Nevertheless, our results can be viewed as an analogy of the linear response theory for the OTOC, as shown in Fig. 2.

5. This theorem can be generalized to finite temperature T case, where

Eq. 14 becomes

$$\exp(-S_A^{(2)}) = \sum_{\hat{M}\in B} \mathrm{Tr}[\hat{M}(t)\hat{O}e^{-\beta\hat{H}}\hat{O}^\dagger\hat{M}(t)\hat{O}e^{-\beta\hat{H}}\hat{O}^\dagger], \tag{15}$$

and the L.H.S. of Eq. 15 approximately equals to the OTOC with temperature $T/2$ as $\mathrm{Tr}[e^{-2\beta\hat{H}}\hat{M}(t)\hat{O}\hat{O}^\dagger\hat{M}(t)\hat{O}\hat{O}^\dagger]$. This theorem can also be generalized to the higher order Rényi entropy.

6. This theorem is quite general. It applies to generic quantum systems, no matter whether they are chaotic, thermalized, localized or not. It builds up a general relation between the OTOC and the Rényi entropy, through which the results obtained from entropy before can be used to infer properties of the OTOC, as we will discuss in the next session 2.2.

2.2 Application on Several Physical Systems

Here we compare three different systems. Let us first introduce the concept of eigen-state thermalization hypothesis (ETH). ETH is defined as follows: for a many-body excited state $|\alpha\rangle$ with energy E_α, dividing the system into two parts of A and B, and suppose $V_\mathrm{A}/V_\mathrm{B} \to 0$ in the thermodynamics limit that both $V_\mathrm{A} \to \infty$ and $V_\mathrm{B} \to \infty$, an ETH is true if

$$\rho_\mathrm{A} = \mathrm{Tr}_\mathrm{B}(|\alpha\rangle\langle\alpha|) = e^{-\hat{H}_\mathrm{A}/(k_\mathrm{b}T_\alpha)}, \tag{16}$$

where $k_\mathrm{b}T_\alpha = E_\alpha$. This immediately implies that if a many-body state obeys ETH, the entropy of its eigenstate will obey volume law. On the contrast, for a localized state, the entropy will obey area law, as only the boundary between A and B contributes to entropy.

In Table 1, "Thermal Phase" denotes a system that obeys ETH. While two localized phases are defined as that do not obey ETH. Here we should stress that since thermalization is a concept for a general excited state, "localized phase" also means that a general excited state is localized. Furthermore, depending on whether there are interaction effects, it can be further distinguished as many-body localized phase (MBL) and single-particle localized phase. It worth emphasizing that, despite of the existence of interaction, that all excited states are still localized is a highly nontrivial statement. That is to say, the existence of MBL phase is a highly nontrivial fact which becomes clear only because of lots of investigations in the past ~ 5 years, and so far the conclusion is clear only in one-dimension.

	Thermal Phase	Many-Body Localized	Single-Particle Localized
Conductivity	May have non-zero DC Conductivity	Zero DC Conductivity	Zero DC Conductivity
ETH	ETH True	ETH False	ETH False
Eigenstates Entanglement	Volume-Law Volume-Law	Area-Law Area-Law	Area-Law Area-Law
Entanglement Spreading	Power-Law Spreading	Logarithmic Spreading	No Spreading
OTOC	Exponential Decay	Power-Law Decay	No Decay

Table 1: A comparison of a "thermal phase" (which means a phase that can thermalize), a many-body localized phase and a single-particle localized phase, in term of DC conductivity, eigen-state thermalization hypothesis (ETH), entanglement entropy of eigenstates, entanglement spreading after a quench and the behavior of OTOC.

As shown in Table 1, the first three raws show that the conductivity, whether ETH is obeyed, or the entropy behavior of the eigenstate can only distinguish the thermal phase from two localized phases, but can not distinguish the many-body localized phase from single-particle localized phase. What can distinguish all three phase is the entropy dynamics after a quench. While our work show that the behavior of the OTOC can also distinguish all of them [16]. Our theorem further reveal that there is a connection between them.

Thermal Phase. We consider the Bose-Hubbard model (BHM) as an example of the thermalized phase, whose Hamiltonian is given by

$$\hat{H} = -J\sum_{\langle ij\rangle}(\hat{b}_i^\dagger\hat{b}_j + \text{h.c.}) + \frac{U}{2}\sum_i \hat{n}_i(\hat{n}_i - 1), \tag{17}$$

where $\hat{b}_i$ is the spinless boson operator at site-i and $\hat{n}_i = \hat{b}_i^\dagger\hat{b}_i$ is the boson number operator. Fig. 3 (A) shows a calculation for $\beta J = 0.9$, $U/J = 10$ with six bosons at six sites in one-dimension. The quench is by removing a boson at the second site, and to calculate the second Rényi entropy, the system is divided into the right and the left three sites. Clearly, it shows that the second Rényi entropy grows linearly after certain time, during the

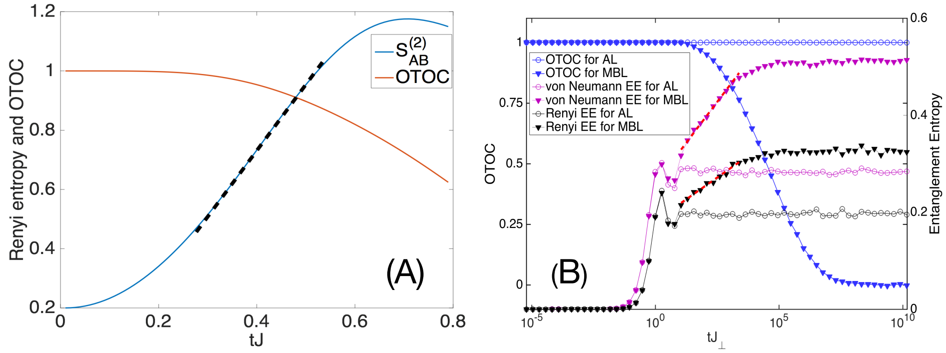

Figure 3: The increasing of the second Rényi entropy after a local quench and the behavior of the OTOC for two local observables for the Bose-Hubbard model, as an example of thermal phase (A), and for XXZ model that exhibits a MBL phase with non-zero J_z and a single-particle localized phase with $J_z = 0$ (B).

same period of time, the decay of the OTOC can be fitted by an exponential function. From the exponential fit, one can further deduce the Lyapunov exponent for the BHM, and in Ref. [27] it is further shown that the Lyapunov exponent will peak at the quantum critical regime.

Localized Phase. We consider the XXZ model as examples for the localized phase [16], whose Hamiltonian is given by

$$\hat{H} = \sum_i J_\perp(\hat{s}_i^x \hat{s}_{i+1}^x + \hat{s}_i^y \hat{s}_{i+1}^y) + J_z \hat{s}_i^z \hat{s}_{i+1}^z + h_i \hat{s}_i^z, \tag{18}$$

where $\hat{s}_i^{x,y,z}$ are three spin operators at site-i, $J_\perp$ and J_z are both constants, and h_i are random fields uniformly distributed among $[-h, h]$. Using a Jordan-Wigner transformation to map this model into a spinless fermion model, $\hat{s}_i^z \hat{s}_{i+1}^z$ gives a nearest neighbour interaction between fermions. Thus in this model, J_z represents the interaction effect. The calculation is done for an 8-site model with open boundary condition, and is averaged over 10^3 disorder configurations. The horizontal axis is $tJ_\perp$ in the logarithmic scale. Here $J_\perp > 0$, $h_i/J_\perp$ is uniformly distributed between $[-5, 5]$. For the MBL case $J_z/J_\perp = 0.2$ where the system is known to be fully localized [31]. For the single-particle localized case $J_z = 0$. For the entropy calculation, the initial state is prepared in a Néel state along $\hat{z}$ direction, and evolves from there under the XXZ Hamiltonian Eq. 18. This initial state preparation can in fact be viewed as a global quench. For the OTOC calculation, we choose $\hat{W}$ as $\hat{s}_x$ at site $i = 2$ and $\hat{V}$ as $\hat{s}_x$ at site $j = 8$. The temperature is also set at infinity and we sum over all configurations with equal weight. In Fig. 3(B), we show that for the MBL phase, the second Rényi entropy grows logarithmically, while during the same period of time, the OTOC decay in a power-law. In fact, this power law behavior can be shown analytically with a phenomenological model for the MBL phase [16]. While for a single-particle localized phase, Fig. 3(B) shows that the second Rényi entropy stop growing after the initial stage, and meanwhile the OTOC remains as a constant. Thus, it shows that the OTOC can distinguish MBL from a single-particle localized phase. As a side remark, it is also easy to show that normal time-ordered correlator can not distinguish them [16].

3 Experimental Measurement of OTOC

3.1 Quantum Simulation

The experimental measurement of OTOC is extremely challenging for two reasons: First, as mentioned above, normal correlator is measured through measuring changing of observables response to perturbation by linear response theory, however, it does not work for the OTOC; Second, if one wants to directly simulate this correlator, it evolves backward evolution in time which requires the controbility of reversing the full Hamiltonian. This is very difficult for most quantum systems.

Therefore, our measurement of OTOC reported in Ref. [28] relies on a quantum simulator. Here our quantum simulator is a NMR on a molecule with four nuclear spins, which can realize any local unitary operation through external control of these nuclear spins. Thus, we can measure any correlator of any four spin Hamiltonian system with this quantum simulation approach.

In this experiment, we focus on a 4-site Ising model with transverse field in both $\hat{x}$ and $\hat{z}$ direction.

$$\hat{H} = \sum_i \left(-\hat{\sigma}_i^z \hat{\sigma}_{i+1}^z + g\hat{\sigma}_i^x + h\hat{\sigma}_i^z \right). \tag{19}$$

When $h = 0$, the Hamiltonian is integrable; while the system is non-integrable when h is finite. Briefly, measurement of OTOC for $\langle \sigma_j^\beta(t) \sigma_i^\alpha \sigma_j^\beta(t) \sigma_i^\alpha \rangle$ follows following three steps:

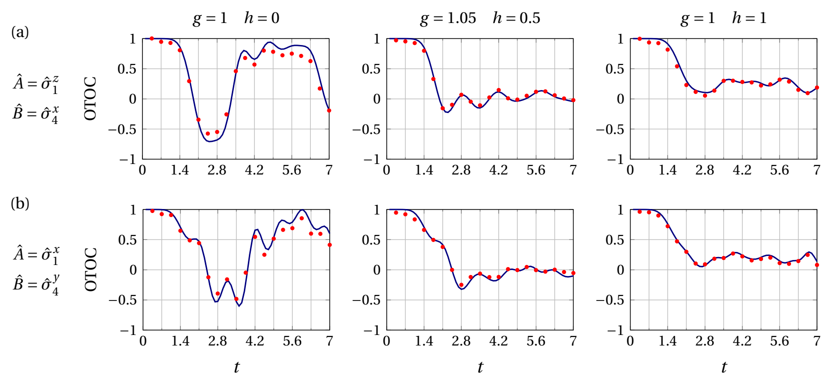

Figure 4: Experimental results of OTOC measurement for an Ising spin chain: (a) $\hat{A} = \hat{\sigma}_1^z$ at the first site, and $\hat{B} = \hat{\sigma}_4^x$ at the fourth site. (b) $\hat{A} = \hat{\sigma}_1^x$ at the first site, and $\hat{B} = \hat{\sigma}_4^y$ at the fourth site. The three columns correspond to $g = 1$, $h = 0$; $g = 1.05$, $h = 0.5$; and $g = 1$, $h = 1$ of model Eq. (19), respectively. The red points are experimental data, the blue curves are theoretical calculation of OTOC with model Eq. (19) for four sites.

1. Initial state preparation. This step aims at preparing an initial state with density matrix $\hat{\rho}_0 \propto \hat{\sigma}_i^\alpha, \alpha = x, y$ or z.

2. Implementing unitary evolution. This step is to simulate a unitary evolution of $\hat{U}(t) = e^{i\hat{H}t}\hat{\sigma}_j^\beta e^{-i\hat{H}t}$ by controlling the nuclear spin with external radio-frequency pulse.

3. Readout. Thus, the density matrix at time t becomes $U(t)\rho_0 U(t)$, and then the OTOC is obtained by measuring the expectation value σ_i^α at time t.

The experimental results are shown in Fig. 4. With our theorem, all OTOC with σ^α at site-i and σ^β at site-j can be measured. Hence, with our theorem, we can determine the entropy dynamics by performing a local quench of spin-flip at site-i, and then considering j-site as part B, we can determine the second Rényi entropy as a function of time. The results are shown in Fig. 5. At the initial stage, extra entropy is generated by the local quench. The difference is manifested in later time. It shows that for an integrable model, the entropy oscillates while for an non-integrable model, the entropy scrambles [14].

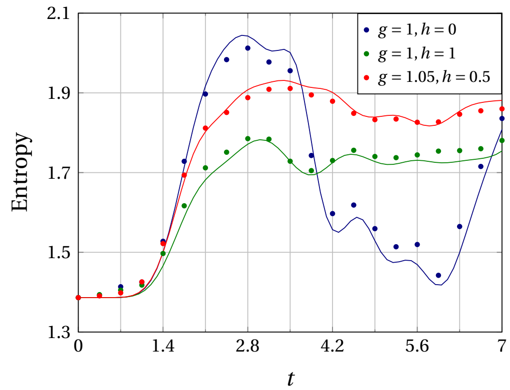

Figure 5: The 2nd Rényi entropy $S_A^{(2)}$ after a quench. A quench operator $(\mathbf{1} + \hat{\sigma}_1^x)$ (up to a normalization factor) is applied to the system at $t = 0$, and the entropy is measured by tracing out the fourth site as the subsystem B. Different colors correspond to different parameters of g and h in the Ising spin model. The points are experimental data, the curves are theoretical calculations.

3.2 Loschmidt Echo

Loschmidt echo is a measurement widely used in many quantum systems, including cold atom system, to quantify how good a revival can occur when an imperfect time-reversal operation is applied to a complex quantum system. Thus it is closely related to the OTOC.

For a pure state $|\Psi\rangle$, the Loschmidt echo is defined as

$$L(t) = |\langle\Psi|e^{i\hat{H}'t}e^{-i\hat{H}t}|\Psi\rangle|^2, \tag{20}$$

where $\hat{H}$ is the Hamiltonian for the forward evolution and $\hat{H}'$ is the Hamiltonian for the backward evolution. Here we consider the special case that $\hat{H}' = \hat{H} + \hat{W}\delta(t - t_0)$, thus $L(t_0)$ is

$$\begin{aligned} L(t_0) &= |\langle\Psi|e^{i\hat{H}t_0}e^{i\hat{W}}e^{-i\hat{H}t_0}|\Psi\rangle|^2 & (21)\\ &= \langle\Psi|e^{i\hat{W}}(t_0)|\Psi\rangle\langle\Psi|e^{i\hat{W}^\dagger}(t_0)|\Psi\rangle & (22)\\ &= \mathrm{Tr}(|\Psi\rangle\langle\Psi|e^{i\hat{W}}(t_0)|\Psi\rangle\langle\Psi|e^{i\hat{W}^\dagger}(t_0)) & (23)\\ &= \mathrm{Tr}(\hat{\rho}e^{i\hat{W}}(t_0)\hat{\rho}e^{i\hat{W}^\dagger}(t_0)). & (24) \end{aligned}$$

That is to say, in this case, the Loschmidt echo is equivalent to a special OTOC between the projection operator $\hat{\rho} = |\Psi\rangle\langle\Psi|$ and another local operator $e^{i\hat{W}}$.

If the initial state is not a pure state but a mixed state described by a density matrix ρ, the Loschmidt echo is defined as

$$\begin{aligned} L(t_0) &= \mathrm{Tr}(e^{-i\hat{H}'t_0}\rho e^{i\hat{H}'t_0}e^{-i\hat{H}t_0}\rho e^{i\hat{H}t_0}) && (25)\\ &= \mathrm{Tr}(\rho e^{i\hat{H}'t_0}e^{-i\hat{H}t_0}\rho e^{i\hat{H}t_0}e^{-i\hat{H}'t_0}) && (26)\\ &= \mathrm{Tr}(\rho e^{i\hat{W}}(t_0)\rho e^{i\hat{W}}(t_0)) && (27) \end{aligned}$$

If we take ρ as a thermal equilibrium suddenly quenched by operator $\hat{O}$, then $\rho = \hat{O}^\dagger e^{-\beta\hat{H}}\hat{O}$, and Eq.27 can be approximated by the OTOC between the operator $e^{i\hat{W}}$ at time t_0 and $\hat{O}^\dagger\hat{O}$ at time $t = 0$.

A Proof of the Theorem

Now we outline how this theorem is proved. For convenience, we first introduce a set of diagrams. For a system divided into subsystems A and B, denote $\{|i\rangle_\mathrm{A} \otimes |i\rangle_\mathrm{B}\}$ as a complete set of bases in the Hilbert space, an arbitrary operator $\hat{Q} = \sum_{ij} Q_{ij}|i\rangle_\mathrm{A} \otimes |i\rangle_\mathrm{B}\langle j|_\mathrm{A} \otimes \langle j|_\mathrm{B}$ is presented diagrammatically in Fig. 6(a1). In this representation, $\mathrm{Tr}_\mathrm{B}\hat{Q}$ can be described by connecting states in the subpart B, as presented by Fig. 6(a2).

Consider a system at $T = \infty$, the initial density matrix $\hat{\rho} \propto \hat{I}$. After the quench by operator $\hat{O}$ and let the system evolve under the Hamiltonian $\hat{H}$ by time t, the density matrix becomes $\hat{\rho} = \hat{U}(t)\hat{O}\hat{O}^\dagger\hat{U}^\dagger(t)$. Then $\hat{\rho}_\mathrm{A}$ will be represented as Fig. 6(b), and straightforwardly, $\mathrm{Tr}\hat{\rho}_\mathrm{A}^2 = e^{-S_\mathrm{A}^{(2)}}$ is presented by Fig. 6(c).

Now we consider each OTOC on the R.H.S. of Eq. 14, which is

$$\begin{aligned} \mathrm{Tr}[\hat{M}(t)\hat{V}(0)\hat{M}(t)\hat{V}(0)] &= \mathrm{Tr}[\hat{U}^\dagger\hat{M}\hat{U}\hat{V}\hat{U}^\dagger\hat{M}\hat{U}\hat{V}]\\ &= \mathrm{Tr}[\hat{U}\hat{V}\hat{U}^\dagger\hat{M}\hat{U}\hat{V}\hat{U}^\dagger\hat{M}]. && (28) \end{aligned}$$

Note that $\hat{V}$ is taken as $\hat{O}\hat{O}^\dagger$ and $\hat{M}$ only acts on the Hilbert space of the subsystem B, this is shown by Fig. 6(d).

Let us again consider a general operator $\hat{Q}$, and sum over a complete set of operators in the subsystem B, since $\sum_{\hat{M}\in B} M_{ij}M_{lm} = \delta_{im}\delta_{lj}$, we will have

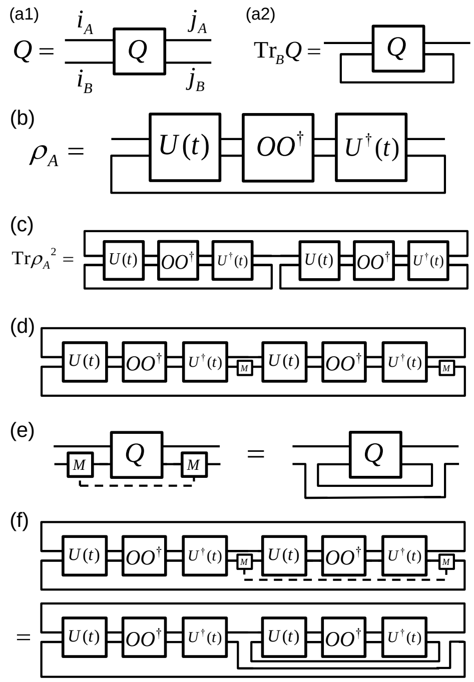

Figure 6: Diagrammatic illustration of how to prove the OTOC-EE theorem. Please see the appendix session A for details.

$\sum_{\hat{M}\in B} \hat{M}\hat{Q}\hat{M} = \mathrm{Tr_B}\hat{Q} \otimes \hat{I}$, which is shown in Fig. 6(e). Finally, applying this identity to $\mathrm{Tr}[\hat{M}(t)\hat{V}(0)\hat{M}(t)\hat{V}(0)]$, the R.H.S. of Eq. 14 is presented in Fig. 6(f). It is clear that the result is equivalent to Fig. 6(c). Hence, we prove the theorem of Eq. 14.

References

[1] A. I. Larkin and Y. N. Ovchinnikov, Sov. Phys. JETP 28, 1200 (1969).

[2] S. H. Shenker and D. Stanford, arXiv:1306.0622.

[3] S. H. Shenker and D. Stanford, arXiv:1312.3296.

[4] A. Kitaev, Hidden correlations in the hawking radiation and thermal noise, (2014), a talk given at Fundamental Physics Prize Symposium, 2014.

[5] S. H. Shenker and D. Stanford, arXiv: 1412.6087.

[6] J. Maldacena, S. H. Shenker, and D. Stanford, arXiv:1503.01409.

[7] A. Kitaev, A simple model of quantum holography, (2015), a talk given at the KITP Program: Entanglement in Strongly-Correlated Quantum Matter, 2015.

[8] J. Maldacena and D. Stanford, arXiv:1604.07818.

[9] S. Banerjee and E. Altman, arXiv:1610.04619.

[10] Y. Gu, X.-L. Qi and D. Stanford, arXiv:1609.07832.

[11] W. Fu, D. Gaiotto, J. Maldacena and S. Sachdev, arXiv:1610.08917.

[12] E. Witten, arXiv:1610.09758.

[13] R. A. Davison, W. Fu, A. Georges, Yingfei Gu, K. Jensen and S. Sachdev, arXiv:1612.00849.

[14] P. Hosur, X L. Qi, D. A. Roberts and B. Yoshida, arXiv:1511.04021.

[15] Y. Huang, Y. L. Zhang and X. Chen, arXiv: 1608.01091.

[16] R. Fan, P. Zhang, H. Shen and H. Zhai arXiv:1608.01914.

[17] Y. Chen, arXiv: 1608.02765.

[18] B. Swingle and D. Chowdhury, arXiv: 1608.03280.

[19] R. Q. He and Z. Y. Lu, arXiv: 1608.03586.

[20] X. Chen, T. Zhou, D. A. Huse and Eduardo Fradkin, arXiv:1610.00220.

[21] D. A. Roberts and B. Yoshida, arXiv:1610.04903.

[22] B. Swingle, G. Bentsen, M. Schleier-Smith and P. Hayden, arXiv:1602.06271.

[23] G. Zhu, M. Hafezi and T. Grover, arXiv:1607.00079.

[24] N. Y. Yao, F. Grusdt, B. Swingle, M. D. Lukin, D. M. Stamper-Kurn, J. E. Moore and E. A. Demler, arXiv:1607.01801.

[25] I. Danshita, M. Hanada and M. Tezuka, arXiv:1606.02454.

[26] L. Álvarez, I. L. Egusquiza, L. Lamata, A. del Campo, J. Sonner and E. Solano1, arXiv:1607.08560v1.

[27] H. Shen, P. Zhang, R. Fan and H. Zhai, arXiv: 1608.02438.

[28] J. Li, R. Fan, H. Wang, B. Ye, B. Zeng, H. Zhai, X. Peng and J. Du, arXiv:1609.01246.

[29] M. Garttner, J. G. Bohnet, A. Safavi-Naini, M. L. Wall, J. J. Bollinger and A. M. Rey, arXiv:1608.08938.

[30] R. Nandkishore and D. Huse, Annu. Rev. Cond. Mat. Phys. **6**, 15 (2015)

[31] A. Pal and D. A. Huse, Phys. Rev. B **82**, 174411 (2010).